

Microscopic description of twisted magnetic Cu_2OSeO_3

Viacheslav A Chizhikov and Vladimir E Dmitrienko

A V Shubnikov Institute of Crystallography, Leninskii pr. 59, 119333 Moscow, Russia

E-mail: chizhikov@crys.ras.ru, dmitrien@crys.ras.ru

Abstract. Twisted structures of chiral cubic ferromagnetics MnSi and Cu_2OSeO_3 can be described both in the frame of the phenomenological Ginzburg–Landau theory and using the microscopical Heisenberg formalism with a chirality brought in by the Dzyaloshinskii–Moriya (DM) interaction. Recent progress in quantum first-principal methods allows to calculate interatomic bond parameters of the Heisenberg model, namely, isotropic exchange constants J_{ij} and DM vectors \mathbf{D}_{ij} , which can be used for simulations of observed magnetic textures and comparison of their calculated characteristics, such as magnetic helix sense and pitch, with the experimental data. In the present work, it is found that unaveraged microscopical details of the spin structures (the local canting) have a strong impact on the global twist and can notably change the helix propagation number. Coefficients \mathcal{J} and \mathcal{D} of the phenomenological theory and helix propagation number $k = \mathcal{D}/2\mathcal{J}$ are derived from interatomic parameters J_{ij} and \mathbf{D}_{ij} of individual bonds for MnSi and Cu_2OSeO_3 crystals and similar cubic magnetics with almost collinear spins.

PACS numbers: 75.25.-j, 75.50.Gg, 75.85.+t, 75.10.Hk

Submitted to: *J. Phys.: Condens. Matter*

1. Introduction

The magnetic properties of the cubic crystal Cu_2OSeO_3 are of great interest for several reasons. First of all, having the space group $P2_13$ without centre of inversion, this crystal becomes a cubic helimagnet below the critical temperature of about 58 K. Moreover, it is the first cubic crystal beyond the class of itinerant magnetics with $B20$ crystal structure [1, 2, 3, 4], for which A-phase, associated with Skyrmion lattice [5, 6, 7], has been recently observed [8, 9, 10, 11, 12, 13]. Secondly, being an insulator, Cu_2OSeO_3 has magnetoelectric properties [13, 14, 15, 16, 17, 18, 19], which provides a new physical significance in comparison with the $B20$ crystals. The interconnection between magnetization gradients and electric polarization makes this crystal potentially applicable for data storing devices and spintronics [20, 21, 22, 23]. And thirdly, but not finally, the more complex than $B20$ structure (16 magnetic copper atoms in two non-equivalent positions in the unit cell) makes it an interesting object for studying the spin textures.

Most of the known twisted magnetics possess symmetry lower than cubic. Their strong anisotropy orients magnetic helices in special crystallographic directions. As opposed to them, in cubic magnetics without centre of inversion, the binding between magnetic and crystal structures can be so subtle, that the helix can be easily reoriented along any direction without essential change of its pitch and energy. Nevertheless, at the microscopic level, this seeming freedom is achieved by correlated tilts of discrete magnetic moments tightly bound with atoms in the crystal. Besides, the easier seems to be the phenomenology of the isotropic system as compared with anisotropic one, the more complex appears its description in terms of discrete spins, particularly when the magnetic helix is oriented by the field in some arbitrary direction. As it has been shown recently for the helimagnetics with $B20$ structure (MnSi-type), this freedom of the helix rotations is achieved by extra tilts (or canting) of the local magnetic moments, which always accompany global spiralling, but are not described in the phenomenological theory. Moreover, the canting still remains, when the spiralling disappears in strong magnetic field.

As a rule, in papers discussing the spin canting some class of canted antiferromagnetics is implied [24], where small relative tilts of magnetic moments belonging to different sublattices result in appearing of weak magnetization. The phenomenon is called weak ferromagnetism, and it serves as direct evidence of the canting, because the tilt angles of individual spins are directly proportional to the observed spontaneous magnetization. The canting in ferromagnetics is less elaborated, and it has been known for many decades that it is more difficult to observe small changes of strong magnetization than small magnetization of weak ferromagnetics. Here, a refined experiment would be useful, e.g. on observation of forbidden Bragg reflections of antiferromagnetic origin [25].

Repeating small rotations (cantings) of spins belonging to neighbouring atomic planes can result in a global twist of crystal magnetization. Therefore, in chiral

ferromagnetics, the twist and the canting are often mistaken for the same thing. Only recently, it was suggested how to distinguish between canting and twist in ferromagnetics [26, 27]. It was shown that the canting should always appear when there are more than one magnetic atom in the unit cell. It leads to coexistence of several spin helices within the helimagnet, which differ by phases and rotational planes (figure 1). It was shown by example of cubic helimagnets with $B20$ structure that the canting makes contribution to the magnetic energy comparable with that of global spiralling. Therefore, it should be taken into account when calculating propagation number of spin helices from the first principles, i.e. starting from the Heisenberg microscopical model of ferromagnetism. Even more intriguing is the fact that, if the Dzyaloshinskii–Moriya (DM) vectors are perpendicular to the bonds between magnetic atoms (which is predicted by many quantum mechanical models), both twist and canting in MnSi-type crystals are determined by the same components of the DM vectors. The study of the Cu_2OSeO_3 crystal, with its structure different from $B20$, also can help us to distinguish between general regularities of twisted cubic magnetics and particularities of the MnSi-type crystals.

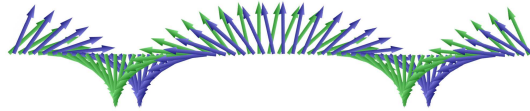


Figure 1. The twist and the canting (by example of a one-dimensional crystal with two magnetic atoms in the unit cell). The canting of spin sublattices leads to the combination of two helices with the same propagation vector and a constant phase shift.

In this paper, a general theory of the spin canting in cubic helimagnetics is developed, which unifies the cases of the MnSi-type and Cu_2OSeO_3 crystals. A microscopical description of the spin structures is made for the case of weakly non-collinear spins. The latter means that the angle between neighbouring spins is close to 0 or to π , i.e. both the spiralling and canting are small. It is just the case of the majority of itinerant magnetics with $B20$ structure (exemplified by MnSi) and twisted ferrimagnetic Cu_2OSeO_3 . We confine ourselves only to the case of the twist induced by the DM interactions; the case of the twist owing to the frustrated exchange is beyond the scope of our consideration. In section 2, the definition of canting is given. Then, the transition to continuous approximation is performed (section 3), and the density of the magnetic energy is calculated (section 4). In section 5, it is shown which simplifications can be made in the case, when, in the absence of the DM interaction, all the spins of the system remain collinear. We assert that two different kinds of the canting exist in the twisted magnetics. The first of them is connected with the gradients of the magnetization, and it arises even in the absence of the DM interaction (in this case the magnetization gradients can be induced by an external influence, e.g. from a surface). In order to take this kind of canting into account, it is convenient to use the method

of fictitious “exchange” coordinates (section 5). Then, simple expressions can be found for the macroscopic constants \mathcal{J} and \mathcal{D} , and the helix propagation number $k = \mathcal{D}/2\mathcal{J}$ (section 6). The second kind of canting is induced by the DM interactions. It can be described in terms of the “tilt” vectors, whose symmetry is found to be determined by the symmetry of the crystal (section 5). The canting of this kind still remains even in the ferromagnetic state, when the helical spin structure is unwound by the external magnetic field. This residual canting can be measured, using neutron and x-ray diffractions (see discussion in section 9). In sections 7 and 8, the theory is applied to the cases of MnSi and Cu_2OSeO_3 , respectively.

2. Balance of magnetic moments and canting

In the classical Heisenberg theory of magnetism, the energy of a magnetic structure is written as

$$E = \sum_i \left\{ \frac{1}{2} \sum_j (-J_{ij} \mathbf{s}_i \cdot \mathbf{s}_j + \mathbf{D}_{ij} \cdot [\mathbf{s}_i \times \mathbf{s}_j]) - \mu_B g_i \mathbf{H} \cdot \mathbf{s}_i \right\}, \quad (1)$$

where i enumerates all the magnetic atoms, the inner sum (j) is taken over close neighbours of i th atom, the coefficient $\frac{1}{2}$ is needed because each bond is included twice in the sum, $\mu_B g_i \mathbf{s}_i$ is the magnetic moment of i th atom (\mathbf{s}_i is the direction of classical spin, $|\mathbf{s}_i| = 1$), J_{ij} are the isotropic exchange constants, whereas the antisymmetrical exchange is characterized by the Dzyaloshinskii–Moriya (DM) vectors \mathbf{D}_{ij} ($J_{ji} = J_{ij}$, $\mathbf{D}_{ji} = -\mathbf{D}_{ij}$), \mathbf{H} is an external magnetic field.

The equation of i th spin balance can be easily found copying out the part of (1) associated with the i th spin,

$$E_i = - \left\{ \sum_j (J_{ij} \mathbf{s}_j + [\mathbf{D}_{ij} \times \mathbf{s}_j]) + \mu_B g_i \mathbf{H} \right\} \cdot \mathbf{s}_i \equiv -\boldsymbol{\varepsilon}_i \cdot \mathbf{s}_i \quad (2)$$

(notice the absence of $\frac{1}{2}$ in comparison with (1)). It is evident that E_i is minimal, when

$$\mathbf{s}_i = \frac{\boldsymbol{\varepsilon}_i}{|\boldsymbol{\varepsilon}_i|}. \quad (3)$$

Being of relativistic origin, the DM interaction is considerably weaker than the isotropic exchange,

$$|\mathbf{D}_{ij}|/J_{ij} \ll 1. \quad (4)$$

Therefore it is convenient to develop a perturbation theory with a small parameter of the order of D/J . In the case of twisted magnetism we can also neglect the influence of the external magnetic field on canting, supposing that

$$H \leq H_{c2} \sim \left(\frac{D}{J} \right)^2 \frac{J}{\mu_B}, \quad (5)$$

where H_{c2} is the field of full “unwinding” of the magnetic helix. Indeed, it has been found in [26] that the energy of canting is of the order of $(D/J)^2$, while the energy of

the interaction of canting with an external magnetic field ($H < H_{c2}$) is determined by the canting of the second order and being proportional to $(D/J)^4$. It follows from the finding of [25] that, in ferromagnetics, the canting of the first order has antiferromagnetic character and does not contribute in this part of the magnetic energy. Notice that, accordingly to the elementary phenomenological theory, the field does not affect the helix pitch, which is in a good agreement with experimental data.

Neglecting the DM interaction and external magnetic field, equation (3) determines an equilibrium system of spins

$$\boldsymbol{\mu}_i \equiv \mathbf{s}_i^{(0)} = \frac{\boldsymbol{\varepsilon}_i^{(0)}}{|\boldsymbol{\varepsilon}_i^{(0)}|}, \quad (6)$$

with

$$\boldsymbol{\varepsilon}_i^{(0)} = |\boldsymbol{\varepsilon}_i^{(0)}| \boldsymbol{\mu}_i = \sum_j J_{ij} \boldsymbol{\mu}_j. \quad (7)$$

The isotropy of the exchange interaction results in that both the structure energy and spin balance remain unchanged, if all the spins rotate as a unit by arbitrary angle relative to immovable atomic structure, or, which is practically the same, if the atomic structure rotates preserving initial spin directions. The latter understanding is important for a cubic crystal structure, where equivalent atomic positions connect to each other by rotational symmetry transformations. It is obvious that a spin balance can be achieved, when $\boldsymbol{\mu}_i$ are equal for all the equivalent positions (figure 2). Here we suppose that the twist is induced only by the DM interactions, and leave the possibility of the pure exchange spiralling outside the scope of our consideration. Notice that such pure exchange twist reveals a threshold behaviour, i.e. it can appear only at some values of the exchange constants.

The non-isotropic DM interaction breaks the symmetry of $\boldsymbol{\mu}_i$, because DM vectors of equivalent bonds change (rotate) with the bond directions. Therefore spin \mathbf{s}_i deviates from $\boldsymbol{\mu}_i$ by a small angle of order of D/J . Taking into account that $|\boldsymbol{\mu}_i| = 1$, this spin change, hereinafter referred to as ‘‘canting’’, in the first approximation is perpendicular to $\boldsymbol{\mu}_i$. Introducing correction $\boldsymbol{\varepsilon}_i^{(1)}$ of first order on D/J , we find

$$\mathbf{s}_i \approx \frac{\boldsymbol{\varepsilon}_i^{(0)} + \boldsymbol{\varepsilon}_{i\parallel}^{(1)} + \boldsymbol{\varepsilon}_{i\perp}^{(1)}}{|\boldsymbol{\varepsilon}_i^{(0)} + \boldsymbol{\varepsilon}_{i\parallel}^{(1)} + \boldsymbol{\varepsilon}_{i\perp}^{(1)}|} \approx \boldsymbol{\mu}_i + \mathbf{u}_i^{(1)} - \frac{|\mathbf{u}_i^{(1)}|^2}{2} \boldsymbol{\mu}_i, \quad (8)$$

where $\boldsymbol{\varepsilon}_{i\parallel}^{(1)}$ and $\boldsymbol{\varepsilon}_{i\perp}^{(1)}$ are parallel and perpendicular to $\boldsymbol{\mu}_i$ components of $\boldsymbol{\varepsilon}_i^{(1)}$, correspondingly; $\mathbf{u}_i^{(1)} \equiv \boldsymbol{\varepsilon}_{i\perp}^{(1)}/|\boldsymbol{\varepsilon}_i^{(0)}|$ is the canting of i th spin in the first approximation, and

$$- \frac{|\mathbf{u}_i^{(1)}|^2}{2} \boldsymbol{\mu}_i \equiv \mathbf{u}_{i\parallel}^{(2)} \quad (9)$$

is proportional to $(D/J)^2$ change of the spin along $\boldsymbol{\mu}_i$ (figure 3).

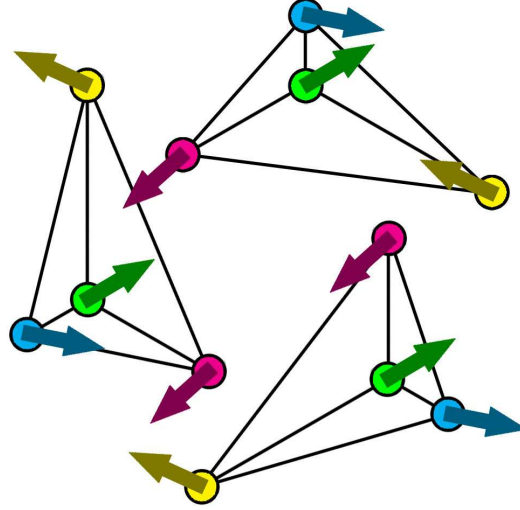


Figure 2. Three magnetic atoms (green) in positions connected by rotational symmetry elements, and their nearest magnetic environments. In absence of non-symmetric DM interaction, a balance is achieved, when the spins in the equivalent positions (equally coloured circles) have the same directions.

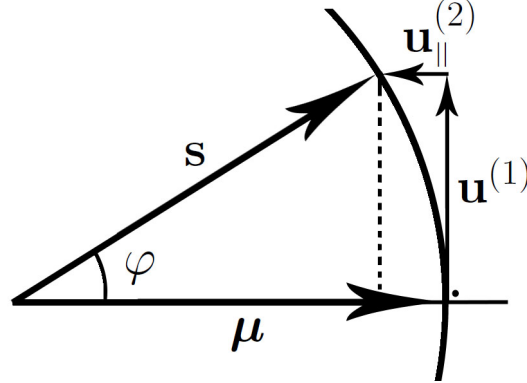


Figure 3. Deviation of spin \mathbf{s} from the equilibrium state $\boldsymbol{\mu}$ in presence of non-isotropic DM interaction. The tilt angle $\varphi \sim D/J$. In a simple approximation the deviation can be decomposed into two parts, $\mathbf{u}^{(1)} \perp \boldsymbol{\mu}$ and $\mathbf{u}_{\parallel}^{(2)} \parallel \boldsymbol{\mu}$.

3. Continuous spin functions

In cubic crystal without centre of inversion, a constant direction of magnetic moment density vector is energetically unfavourable, and magnetic structure becomes twisted. Besides, the strength of the twist is characterized by the same ratio D/J as the canting does. If the magnetic moment density changes slowly along the crystal, a transition can be performed from discrete spins to smooth continuous spin functions $\hat{\mathbf{s}}_i(\mathbf{r})$, whose number coincides with the number of magnetic atoms in the crystal unit cell. Then, the

magnetic energy can be rewritten in integral form [27],

$$E = \int d\mathbf{r} \sum_i \left\{ \frac{1}{2} \sum_j (-J_{ij} \hat{\mathbf{s}}_i \cdot \exp(\mathbf{b}_{ij} \cdot \nabla) \hat{\mathbf{s}}_j + \mathbf{D}_{ij} \cdot [\hat{\mathbf{s}}_i \times \exp(\mathbf{b}_{ij} \cdot \nabla) \hat{\mathbf{s}}_j]) - \mu_B g_i \mathbf{H} \cdot \hat{\mathbf{s}}_i \right\}, \quad (10)$$

where the sum (i) is now taken over all the magnetic atoms in the unit cell, and \mathbf{b}_{ij} is a bond directed from i th to j th atom; both \mathbf{r} and \mathbf{b}_{ij} are measured in cubic cell parameters $a = 1$; the values of the spin functions and their spatial derivatives in the integrand are taken at the same point.

Using (2), the vector $\hat{\boldsymbol{\varepsilon}}_i^{(1)}(\mathbf{r})$ can be written in continuous approximation,

$$\hat{\boldsymbol{\varepsilon}}_i^{(1)} = \sum_j \left(J_{ij} \hat{\mathbf{u}}_j^{(1)} + J_{ij} (\mathbf{b}_{ij} \cdot \nabla) \hat{\boldsymbol{\mu}}_j + [\mathbf{D}_{ij} \times \hat{\boldsymbol{\mu}}_j] \right), \quad (11)$$

where we neglect the magnetic field and replace $\mathbf{u}_j^{(1)}$ and $\boldsymbol{\mu}_j$ with continuous functions $\hat{\mathbf{u}}_j^{(1)}(\mathbf{r})$ and $\hat{\boldsymbol{\mu}}_j(\mathbf{r})$. Here, we use condition (4) and make the expansion, assuming that not only canting in the first approximation but also the global gradients of the magnetic structure (e.g. the helix propagation number) are determined by small parameter D/J , i.e. $\nabla \sim k \sim D/J$. Then,

$$|\hat{\boldsymbol{\varepsilon}}_i^{(0)}| \hat{\mathbf{u}}_i^{(1)} = \left\{ \sum_j \left(J_{ij} \hat{\mathbf{u}}_j^{(1)} + J_{ij} (\mathbf{b}_{ij} \cdot \nabla) \hat{\boldsymbol{\mu}}_j + [\mathbf{D}_{ij} \times \hat{\boldsymbol{\mu}}_j] \right) \right\}_{\perp}, \quad (12)$$

where the subscript “ \perp ” designates vector projection on the plane perpendicular to $\hat{\boldsymbol{\mu}}_i$. Because $\hat{\mathbf{u}}_j^{(1)} \perp \hat{\boldsymbol{\mu}}_j$ and $|\hat{\boldsymbol{\mu}}_j| = 1$, then each summand in the sum over j is a vector perpendicular to $\hat{\boldsymbol{\mu}}_j$. Equation (12) shows that the canting is determined by both the DM interaction and spatial derivatives of $\hat{\boldsymbol{\mu}}$.

Let us average out (12) using the crystal symmetry. For any cubic (or tetrahedral) point group

$$\langle \mathbf{b}_{ij} \rangle_{\text{eq}} = \langle \mathbf{D}_{ij} \rangle_{\text{eq}} = 0, \quad (13)$$

where index “eq” means averaging over equivalent bonds and positions. Thus, we obtain

$$|\hat{\boldsymbol{\varepsilon}}_i^{(0)}| \langle \hat{\mathbf{u}}_i^{(1)} \rangle_{\text{eq}} = \sum_j J_{ij} \langle \hat{\mathbf{u}}_j^{(1)} \rangle_{\text{eq}, \perp}. \quad (14)$$

It is evident from comparison with (7), that condition (14) is satisfied, when

$$\langle \hat{\mathbf{u}}_i^{(1)} \rangle_{\text{eq}} = [\boldsymbol{\varphi} \times \hat{\boldsymbol{\mu}}_i], \quad (15)$$

with $[\boldsymbol{\varphi} \times \hat{\boldsymbol{\mu}}_i]$ being the change of spin $\hat{\boldsymbol{\mu}}_i$, induced by rotation of all the spins as a unit by a small angle $\boldsymbol{\varphi}$. As is mentioned above, the rotation does not change the isotropic exchange energy and results in new functions $\hat{\boldsymbol{\mu}}_i$, also satisfying (7). Therefore it is possible to include $\langle \hat{\mathbf{u}}_i^{(1)} \rangle_{\text{eq}}$ into the definition of $\hat{\boldsymbol{\mu}}_i$ and assume without loss of generality that

$$\langle \hat{\mathbf{u}}_i^{(1)} \rangle_{\text{eq}} = 0. \quad (16)$$

In this case, $\hat{\boldsymbol{\mu}}_i$ is the normalized average spin over all the positions in the unit cell equivalent to the i th one.

4. Energy of twist and canting

Let us write out the contributions to the energy (10) up to the second order terms on D/J . The zero order energy is

$$\mathcal{E}^{(0)} = -\frac{1}{2} \sum_i \sum_j J_{ij} \hat{\boldsymbol{\mu}}_i \cdot \hat{\boldsymbol{\mu}}_j. \quad (17)$$

The 1st order contribution

$$\begin{aligned} \mathcal{E}^{(1)} = \frac{1}{2} \sum_i \sum_j \left\{ -J_{ij} \left(\hat{\boldsymbol{\mu}}_i \cdot (\mathbf{b}_{ij} \cdot \nabla) \hat{\boldsymbol{\mu}}_j \right. \right. \\ \left. \left. + \hat{\mathbf{u}}_i^{(1)} \cdot \hat{\boldsymbol{\mu}}_j + \hat{\boldsymbol{\mu}}_i \cdot \hat{\mathbf{u}}_j^{(1)} \right) + \mathbf{D}_{ij} \cdot [\hat{\boldsymbol{\mu}}_i \times \hat{\boldsymbol{\mu}}_j] \right\} \end{aligned} \quad (18)$$

becomes zero in the equilibrium due to (13) and (16).

It is convenient to divide the 2nd order contribution into two parts: the first one, associated with the gradients of the magnetic moment $\hat{\boldsymbol{\mu}}$ only,

$$\begin{aligned} \mathcal{E}_\mu^{(2)} = \frac{1}{2} \sum_i \sum_j \left\{ -\frac{1}{2} J_{ij} \hat{\boldsymbol{\mu}}_i \cdot (\mathbf{b}_{ij} \cdot \nabla)^2 \hat{\boldsymbol{\mu}}_j \right. \\ \left. + \mathbf{D}_{ij} \cdot [\hat{\boldsymbol{\mu}}_i \times (\mathbf{b}_{ij} \cdot \nabla) \hat{\boldsymbol{\mu}}_j] \right\}, \end{aligned} \quad (19)$$

and the second one, depending on local cantings,

$$\begin{aligned} \mathcal{E}_u^{(2)} = \frac{1}{2} \sum_i \sum_j \left\{ -J_{ij} \left(\hat{\mathbf{u}}_i^{(2)} \cdot \hat{\boldsymbol{\mu}}_j + \hat{\boldsymbol{\mu}}_i \cdot \hat{\mathbf{u}}_j^{(2)} \right. \right. \\ \left. \left. + \hat{\mathbf{u}}_i^{(1)} \cdot (\mathbf{b}_{ij} \cdot \nabla) \hat{\boldsymbol{\mu}}_j - \hat{\mathbf{u}}_j^{(1)} \cdot (\mathbf{b}_{ij} \cdot \nabla) \hat{\boldsymbol{\mu}}_i \right. \right. \\ \left. \left. + \hat{\mathbf{u}}_i^{(1)} \cdot \hat{\mathbf{u}}_j^{(1)} \right) + \mathbf{D}_{ij} \cdot \left([\hat{\mathbf{u}}_i^{(1)} \times \hat{\boldsymbol{\mu}}_j] + [\hat{\boldsymbol{\mu}}_i \times \hat{\mathbf{u}}_j^{(1)}] \right) \right\}. \end{aligned} \quad (20)$$

The expression for $\mathcal{E}_\mu^{(2)}$ can be averaged over equivalent bonds, using equation

$$\langle a_\alpha b_\beta \rangle_{\text{eq}} = \frac{1}{3} \delta_{\alpha\beta} (\mathbf{a} \cdot \mathbf{b}) \quad (21)$$

for the vectors \mathbf{a} and \mathbf{b} transformed with the elements of the cubic (tetrahedral) point group. Then

$$\begin{aligned} \mathcal{E}_\mu^{(2)} = -\frac{1}{6} \sum_i \sum_j \left\{ \frac{1}{2} J_{ij} |\mathbf{b}_{ij}|^2 \hat{\boldsymbol{\mu}}_i \cdot \Delta \hat{\boldsymbol{\mu}}_j \right. \\ \left. + (\mathbf{D}_{ij} \cdot \mathbf{b}_{ij}) \hat{\boldsymbol{\mu}}_i \cdot [\nabla \times \hat{\boldsymbol{\mu}}_j] \right\}. \end{aligned} \quad (22)$$

Notice that all the summands corresponding to equivalent bonds are equal, and, therefore, we can calculate them only once, multiplying then by the bond multiplicities.

Changing summation order and using relations $\mathbf{b}_{ji} = -\mathbf{b}_{ij}$ and $\mathbf{D}_{ji} = -\mathbf{D}_{ij}$, equation (20) can be rewritten as

$$\mathcal{E}_u^{(2)} = \sum_i \sum_j \left\{ -J_{ij} \left(\hat{\mathbf{u}}_i^{(2)} \cdot \hat{\boldsymbol{\mu}}_j + \hat{\mathbf{u}}_i^{(1)} \cdot (\mathbf{b}_{ij} \cdot \nabla) \hat{\boldsymbol{\mu}}_j + \frac{1}{2} \hat{\mathbf{u}}_i^{(1)} \cdot \hat{\mathbf{u}}_j^{(1)} \right) + \mathbf{D}_{ij} \cdot [\hat{\mathbf{u}}_i^{(1)} \times \hat{\boldsymbol{\mu}}_j] \right\}. \quad (23)$$

Using (7), (9) and (12), the latter expression can be transformed to

$$\mathcal{E}_u^{(2)} = -\frac{1}{2} \sum_i |\hat{\boldsymbol{\epsilon}}_i^{(0)}| |\hat{\mathbf{u}}_i^{(1)}|^2 + \frac{1}{2} \sum_i \sum_j J_{ij} \hat{\mathbf{u}}_i^{(1)} \cdot \hat{\mathbf{u}}_j^{(1)}. \quad (24)$$

5. The case of collinear mean spins

In frustrated magnetic structures, the spins $\hat{\boldsymbol{\mu}}_i$ can be non-collinear. Besides, in a number of practically important cases, including ferro-, antiferro-, and some ferrimagnetic orders, all $\hat{\boldsymbol{\mu}}_i$ can be aligned along a line, and several considerable simplifications can be made. Indeed, assume that

$$\hat{\boldsymbol{\mu}}_i = c_i \hat{\boldsymbol{\mu}} \quad c_i = \pm 1 \quad |\hat{\boldsymbol{\mu}}| = 1. \quad (25)$$

Here, $\hat{\boldsymbol{\mu}}$ is a unit vector directed along the local magnetization. Then all $\hat{\mathbf{u}}_i^{(1)}$ belong to the plane perpendicular to $\hat{\boldsymbol{\mu}}$, and we can discard the index “ \perp ” in (12):

$$\left| \sum_j J_{ij} c_j \right| \hat{\mathbf{u}}_i^{(1)} = \sum_j \left\{ J_{ij} \hat{\mathbf{u}}_j^{(1)} + J_{ij} c_j (\mathbf{b}_{ij} \cdot \nabla) \hat{\boldsymbol{\mu}} + c_j [\mathbf{D}_{ij} \times \hat{\boldsymbol{\mu}}] \right\}, \quad (26)$$

where is used that

$$|\hat{\boldsymbol{\epsilon}}_i^{(0)}| = \left| \sum_j J_{ij} c_j \right|. \quad (27)$$

Another simplification is the use of condition

$$\sum_j J_{ij} c_j \mathbf{b}_{ij} = 0. \quad (28)$$

The system (28) contains several independent vector equations (whose number coincides with the number of non-equivalent magnetic positions in the unit cell) and can be considered as a condition imposed on the atomic coordinates. Indeed, the energy (1) does not depend explicitly on the atomic coordinates, as opposed to expression (10), where they are included in vectors \mathbf{b}_{ij} . Obviously, the coordinates should disappear after minimization of the energy, therefore we can choose them arbitrarily, e.g. using condition (28). It is shown in [27], that the possibility of intentional choice of ideal atomic coordinates is connected with the ambiguity of transition from discrete spins to continuous density of magnetic moment. Notice that, because (28) contains only exchange interaction parameters, these fictitious coordinates depend only on J_{ij} . So,

hereinafter we will refer to the positions as “exchange” ones. In section 9 the sense and properties of the exchange coordinates are discussed in details.

The atomic “shift” from real to fictitious positions results in disappearing of the part of the canting induced by derivatives of $\hat{\boldsymbol{\mu}}$:

$$\left| \sum_j J_{ij} c_j \right| \hat{\mathbf{u}}_i^{(1)} = \sum_j \left(J_{ij} \hat{\mathbf{u}}_j^{(1)} + c_j [\mathbf{D}_{ij} \times \hat{\boldsymbol{\mu}}] \right). \quad (29)$$

Now the canting can be found in form

$$\hat{\mathbf{u}}_i^{(1)} = c_i [\boldsymbol{\rho}_i \times \hat{\boldsymbol{\mu}}], \quad (30)$$

where “tilt” vectors $\boldsymbol{\rho}_i$ possess the following properties. (i) The vector $\boldsymbol{\rho}_i$ corresponds to the symmetry of the i th atomic position, e.g. the tilt vector of an atom in position $4a$ of the space group $P2_13$ is directed along 3-fold axis of symmetry passing through the atom, whereas the tilt vector of an atom in position $12b$ has three independent components. (ii) The tilt vectors in equivalent positions are connected to each other by the corresponding transformation of the point group.

Now the system (29) can be rewritten as

$$\left| \sum_j J_{ij} c_j \right| c_i \boldsymbol{\rho}_i = \sum_j (J_{ij} c_j \boldsymbol{\rho}_j + c_j \mathbf{D}_{ij}). \quad (31)$$

The system (31) contains as many independent vector equations as many non-equivalent magnetic atoms are in the unit cell.

6. Phenomenological constants

The energy density expressions are also simplified in the case of collinear mean spins:

$$\mathcal{E}^{(0)} = -\frac{1}{2} \sum_i \sum_j J_{ij} c_i c_j, \quad (32)$$

$$\begin{aligned} \mathcal{E}_\mu^{(2)} = & -\frac{1}{12} \left(\sum_i \sum_j J_{ij} c_i c_j |\mathbf{b}_{ij}|^2 \right) \hat{\boldsymbol{\mu}} \cdot \Delta \hat{\boldsymbol{\mu}} \\ & -\frac{1}{6} \left(\sum_i \sum_j c_i c_j \mathbf{D}_{ij} \cdot \mathbf{b}_{ij} \right) \hat{\boldsymbol{\mu}} \cdot [\nabla \times \hat{\boldsymbol{\mu}}]. \end{aligned} \quad (33)$$

Using equation

$$\langle [\boldsymbol{\rho}_i \times \hat{\boldsymbol{\mu}}] \cdot [\boldsymbol{\rho}_j \times \hat{\boldsymbol{\mu}}] \rangle_{\text{eq}} = \frac{2}{3} \boldsymbol{\rho}_i \cdot \boldsymbol{\rho}_j, \quad (34)$$

we find

$$\mathcal{E}_u^{(2)} = -\frac{1}{3} \sum_i \left| \sum_j J_{ij} c_j \right| |\boldsymbol{\rho}_i|^2 + \frac{1}{3} \sum_i \sum_j J_{ij} c_i c_j \boldsymbol{\rho}_i \cdot \boldsymbol{\rho}_j \quad (35)$$

or, using (31),

$$\mathcal{E}_u^{(2)} = -\frac{1}{3} \sum_i \sum_j c_i c_j \mathbf{D}_{ij} \cdot \boldsymbol{\rho}_i. \quad (36)$$

Notice that in the latter expression as well as in (33) the summands corresponding to equivalent bonds are equal. In the given approximation, expression (36) is nothing but a constant (negative) addition to the magnetic energy. However, it was found in [27] that this contribution had view $f(M) \sim \sqrt{M_0^2 - M^2}$, with M_0 being a saturation magnetization. This term is important for describing of double twisted magnetic structures, e.g. the Skyrmion lattices (A-phases) and hypothetical cubic textures similar to the blue phases of liquid crystals. Indeed, it is not clear so far why the A-phases are energetically preferable in some ranges of temperatures and magnetic fields. In order to solve this problem, in the phenomenological theory, they often add to the energy a correction term in the form $f(M) \sim aM^2 + bM^4$. Yet a trouble emerges here, namely, the magnetization in some areas can exceed the saturation value M_0 . The form $f(M) \sim \sqrt{M_0^2 - M^2}$, resulting from the Heisenberg model, resolves this difficulty.

Because, as is seen from (31), $\boldsymbol{\rho}_i$ are independent of spatial derivatives of $\hat{\boldsymbol{\mu}}$, the energy $\mathcal{E}_u^{(2)}$ does not contain the derivatives as well. On the other hand, $\mathcal{E}_\mu^{(2)}$ does not depend on $\boldsymbol{\rho}_i$, and this part of the energy can be rewritten in the following form conventional for the macroscopic phenomenological theory

$$\mathcal{E}_\mu^{(2)} = \mathcal{J} \frac{\partial \hat{\mu}_i}{\partial x_k} \frac{\partial \hat{\mu}_i}{\partial x_k} + \mathcal{D} \hat{\boldsymbol{\mu}} \cdot [\nabla \times \hat{\boldsymbol{\mu}}], \quad (37)$$

where \mathcal{J} and \mathcal{D} are the phenomenological constants expressed now through the parameters of the microscopical Heisenberg model:

$$\mathcal{J} = \frac{1}{12} \sum_i \sum_j J_{ij} c_i c_j |\mathbf{b}_{ij}|^2, \quad (38)$$

$$\mathcal{D} = -\frac{1}{6} \sum_i \sum_j c_i c_j \mathbf{D}_{ij} \cdot \mathbf{b}_{ij}, \quad (39)$$

and $\hat{\boldsymbol{\mu}}$ is a unit vector oriented along the local magnetic moment density \mathbf{M} . Parameters \mathcal{J} and \mathcal{D} determine spiralling of the spin structure. In particular, the minimization of (37) gives as a result the helix with propagation number

$$k = \frac{\mathcal{D}}{2\mathcal{J}} \quad (40)$$

and vector $\hat{\boldsymbol{\mu}}$ rotating in the plane perpendicular to the helix axis.

The absence of canting in expression (37) does not mean that the canting does not affect the spiralling. As a matter of fact, the contribution of canting is taken into account, when choosing the fictitious atomic coordinates with condition (28). The simple additive expressions (38) and (39) can appear only because the contributing bonds \mathbf{b}_{ij} are the functions of the exchange coordinates. Notice that, due to the dependence of vectors \mathbf{b}_{ij} on the exchange constants, both \mathcal{J} and \mathcal{D} are non-linear functions of J_{ij} . In the case of n non-equivalent bonds with parameters $J_1 \dots J_n$,

$\mathbf{D}_1 \dots \mathbf{D}_n$ and m independent coordinates of magnetic atoms ($m = 1$ for MnSi and $m = 4$ for Cu_2OSeO_3), the phenomenological constants have the following views: $\mathcal{J} = P_{2m+1}(J_1 \dots J_n)/P_m^2(J_1 \dots J_n)$, $\mathcal{D} = P_{1,m}(\mathbf{D}_1 \dots \mathbf{D}_n, J_1 \dots J_n)/P_m(J_1 \dots J_n)$, where P_{2m+1} and P_m are some homogeneous polynomials of $J_1 \dots J_n$ with degrees $2m+1$ and m , correspondingly, and $P_{1,m}$ is a homogeneous polynomial linear by the components of vectors $\mathbf{D}_1 \dots \mathbf{D}_n$ and being of degree m with respect to $J_1 \dots J_n$. Indeed, it follows from equation (28), which is a system of m linear equations with respect exchange coordinates, with both coefficients and constant terms being linear functions of $J_1 \dots J_n$. Consequently, the intuitively obvious for dimensional reason expression $k \sim D/J$ transforms to $k \sim P_{1,m}(\mathbf{D}_1 \dots \mathbf{D}_n, J_1 \dots J_n)P_m(J_1 \dots J_n)/P_{2m+1}(J_1 \dots J_n)$.

7. The example of the MnSi-type crystals

Let us illustrate the theory developed by a simple example of the MnSi-type crystals with the $B20$ structure. The cubic crystal MnSi has the space group $P2_13$. Its unit cell contains four magnetic manganese atoms in the position $4a$ (at threefold axes) with $x = 0.138$. In accordance with [27], we define four magnetic shells by the non-equivalent bonds $\mathbf{b}_1 = (-2x, \frac{1}{2}, \frac{1}{2} - 2x)$, $\mathbf{b}_2 = (1 - 2x, \frac{1}{2}, \frac{1}{2} - 2x)$, $\mathbf{b}_3 = (-2x, \frac{1}{2}, -\frac{1}{2} - 2x)$, and $\mathbf{b}_4 = (1, 0, 0)$, with corresponding exchange constants J_1 – J_4 and DM vectors \mathbf{D}_1 – \mathbf{D}_4 .

The first atom (x, x, x) has 6 bonds of each kind: $(-2x, \pm\frac{1}{2}, \frac{1}{2} - 2x) \odot$, $(1 - 2x, \pm\frac{1}{2}, \frac{1}{2} - 2x) \odot$, $(-2x, \pm\frac{1}{2}, -\frac{1}{2} - 2x) \odot$, $\pm(1, 0, 0) \odot$ (the symbol \odot means possible cyclic permutations of the coordinates). The corresponding DM vectors can be obtained from \mathbf{D}_1 – \mathbf{D}_4 by the same sing changes and cyclic permutations of the components.

We assign $c_i = 1$ for all the manganese atoms in the equivalent positions. Then, condition (28) for the atom (x, x, x) can be rewritten as

$$\sum_j J_{ij} \mathbf{b}_{ij} = 0 \quad (41)$$

or, using the symmetry 3 of the position,

$$J_1 \left(\frac{1}{2} - 4x \right) + J_2 \left(\frac{3}{2} - 4x \right) + J_3 \left(-\frac{1}{2} - 4x \right) + J_4 \cdot 0 = 0 \quad (42)$$

and

$$x_{\text{exch}} = \frac{J_1 + 3J_2 - J_3}{8(J_1 + J_2 + J_3)} \quad (43)$$

in accordance with [27]. The 4th neighbours do not influence the exchange coordinate, because the bond \mathbf{b}_4 connect the atoms belonging to the same magnetic sublattice.

From (38) and (39) the macroscopic parameters can be found,

$$\mathcal{J} = 2(J_1 b_1^2 + J_2 b_2^2 + J_3 b_3^2 + J_4 b_4^2), \quad (44)$$

$$\mathcal{D} = -4(\mathbf{D}_1 \cdot \mathbf{b}_1 + \mathbf{D}_2 \cdot \mathbf{b}_2 + \mathbf{D}_3 \cdot \mathbf{b}_3 + \mathbf{D}_4 \cdot \mathbf{b}_4). \quad (45)$$

After substitution of the exchange coordinate x_{exch} into the \mathbf{b} vectors, the macroscopic exchange parameter can be expressed through the exchange constants of the bonds,

$$\mathcal{J} = \frac{3J_1^2 + 3J_2^2 + 3J_3^2 + 10J_1J_2 + 10J_1J_3 + 22J_2J_3}{4(J_1 + J_2 + J_3)} + 2J_4, \quad (46)$$

which coincides with the result from [27].

The atom (x, x, x) , belonging to the 1st magnetic sublattice of the crystal, has two atoms of each other sublattice (2, 3, 4) in the 1st, the 2nd and the 3rd magnetic coordination spheres, and six atoms of the same sublattice (1) in the 4th coordination sphere. Therefore, condition (31) on tilt vectors can be written for the atom (x, x, x) as

$$6(J_1 + J_2 + J_3 + J_4)\boldsymbol{\rho}_1 = 2(J_1 + J_2 + J_3)(\boldsymbol{\rho}_2 + \boldsymbol{\rho}_3 + \boldsymbol{\rho}_4) + 6J_4\boldsymbol{\rho}_1 + 2D_+(1, 1, 1), \quad (47)$$

with $D_+ = D_{1x} + D_{1z} + D_{2x} + D_{2z} + D_{3x} + D_{3z}$. Using symmetry equation

$$\boldsymbol{\rho}_1 + \boldsymbol{\rho}_2 + \boldsymbol{\rho}_3 + \boldsymbol{\rho}_4 = 0, \quad (48)$$

we find

$$\boldsymbol{\rho}_1 = (\rho_x, \rho_x, \rho_x) \quad \rho_x = \frac{D_+}{4(J_1 + J_2 + J_3)} \quad (49)$$

in accordance with [27]. Tilt vectors $\boldsymbol{\rho}_2$, $\boldsymbol{\rho}_3$ and $\boldsymbol{\rho}_4$ of other manganese atoms in the unit cell can be obtained from $\boldsymbol{\rho}_1$ by the corresponding symmetry transformations. As is seen from (49), the 4th magnetic neighbours, belonging to the same sublattice, do not influence tilt vectors.

8. The case of Cu_2OSeO_3

The cubic crystal Cu_2OSeO_3 has the space group $P2_13$, the lattice constant $a = 8.925$ Å. Its unit cell contains 16 magnetic copper atoms: four Cu-I in the position $4a$ with coordinates $\mathbf{r}_I = (x_I, x_I, x_I) = (0.8860, 0.8860, 0.8860)$ (at threefold axes) and twelve Cu-II in the general position $12b$ with coordinates $\mathbf{r}_{II} = (0.1335, 0.1211, 0.8719)$ [28]. In the unit cell, 16 copper atoms form four almost regular tetrahedra, which, in their turn, do a bigger one, resembling the first-order model of the Sierpinski fractal tetrahedron (figure 4). All the bonds shown by the rods in the picture have approximately the same length. The nearest magnetic environment is determined by four types of non-equivalent bonds, but following [19] we take into account an additional bond with the atoms of the second magnetic environment. The examples of these five non-equivalent bonds are represented by the arrows in figure 4. In table 1, the coordinates and the energetic parameters are listed of five non-equivalent bonds, radiated from the Cu-II atom in position \mathbf{r}_{II} .

The magnetic neighbours of atom Cu-I are nine copper atoms in positions $12b$. Three of them are listed in table 2. Because the atom in position \mathbf{r}_I is on the 3-fold axis [111], the remaining six bonds can be obtained by cyclic permutations of the coordinates of the vectors.

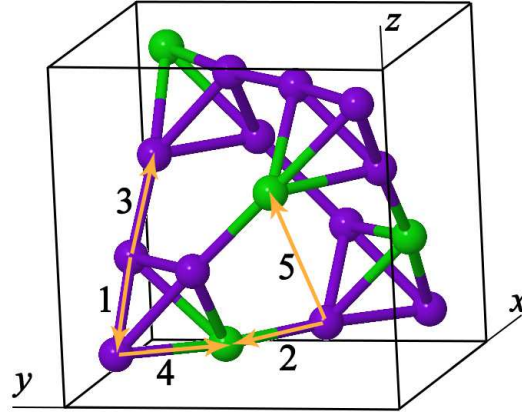


Figure 4. Copper atoms in the unit cell of Cu_2OSeO_3 : four Cu-I (green) in positions $4a$ and twelve Cu-II (indigo) in positions $12b$ of the space group $P2_13$. The arrows show five non-equivalent bonds providing main contributions into the isotropic exchange and the DM interactions.

Table 1. Cu_2OSeO_3 crystal: five non-equivalent bonds between copper atoms with the corresponding exchange constants J and DM vectors \mathbf{D} , taken from [19]. The lattice parameter $a = 8.925\text{\AA}$ and atomic coordinates are as in [28].

$\mathbf{b} + (x_{\text{II}}, y_{\text{II}}, z_{\text{II}})$	$a \mathbf{b} , \text{\AA}$	J, meV	\mathbf{D}, meV
$-\frac{1}{2} + z_{\text{II}}, \frac{1}{2} - x_{\text{II}}, 1 - y_{\text{II}}$	3.054	$J_1 = 1.132$	$\mathbf{D}_1 = (0.289, -0.325, -0.051)$
$-1 + x_{\text{I}}, -1 + x_{\text{I}}, x_{\text{I}}$	3.049	$J_2 = -6.534$	$\mathbf{D}_2 = (1.12, -1.376, 0.300)$
$-1 + z_{\text{II}}, x_{\text{II}}, 1 + y_{\text{II}}$	3.226	$J_3 = 3.693$	$\mathbf{D}_3 = (-0.263, 0.167, -0.407)$
$1 - x_{\text{I}}, -\frac{1}{2} + x_{\text{I}}, \frac{3}{2} - x_{\text{I}}$	3.304	$J_4 = -0.900$	$\mathbf{D}_4 = (-0.490, 1.238, 1.144)$
$\frac{1}{2} - x_{\text{I}}, 1 - x_{\text{I}}, -\frac{1}{2} + x_{\text{I}}$	6.349	$J_5 = -0.984$	$\mathbf{D}_5 = (0.045, -0.087, -0.059)$

Table 2. Magnetic neighbours of copper Cu-I in position \mathbf{r}_{I} , energy parameters of the bonds and tilt vectors $\boldsymbol{\rho}$. Only three neighbours are listed. Other six bonds can be obtained by threefold rotations, i.e. by cyclic permutations of the coordinates of the vectors.

$\mathbf{r}_j = \mathbf{r}_{\text{I}} + \mathbf{b}_{ij}$	J_{ij}	\mathbf{D}_{ij}	$\boldsymbol{\rho}_j$
$1 + x_{\text{II}}, 1 + y_{\text{II}}, z_{\text{II}}$	J_2	$-D_{2x}, -D_{2y}, -D_{2z}$	$\rho_{\text{II},x}, \rho_{\text{II},y}, \rho_{\text{II},z}$
$1 - x_{\text{II}}, \frac{1}{2} + y_{\text{II}}, \frac{3}{2} - z_{\text{II}}$	J_4	$D_{4x}, -D_{4y}, D_{4z}$	$-\rho_{\text{II},x}, \rho_{\text{II},y}, -\rho_{\text{II},z}$
$\frac{1}{2} - x_{\text{II}}, 1 - y_{\text{II}}, \frac{1}{2} + z_{\text{II}}$	J_5	$D_{5x}, D_{5y}, -D_{5z}$	$-\rho_{\text{II},x}, -\rho_{\text{II},y}, \rho_{\text{II},z}$

The magnetic environment of atom Cu-II contains seven copper atoms: four in positions $12b$ and three in positions $4a$ (table 3).

All 16 copper positions in the unit cell are characterized by “sense” numbers c_i and tilt vectors $\boldsymbol{\rho}_i$ determining canting. Owing to ferrimagnetic order, the spins of the copper atoms in positions $4a$ are opposite to those in positions $12b$ and to the summary magnetic moment [14], so we can assign the values $c_{\text{I}} = -1$ and $c_{\text{II}} = 1$. The tilt vectors of the atoms in positions \mathbf{r}_{I} and \mathbf{r}_{II} are chosen as $(\rho_{\text{I},x}, \rho_{\text{I},x}, \rho_{\text{I},x})$ and $(\rho_{\text{II},x}, \rho_{\text{II},y}, \rho_{\text{II},z})$,

Table 3. Magnetic neighbours of copper Cu-II in position \mathbf{r}_{II} , energy parameters of the bonds and tilt vectors $\boldsymbol{\rho}$.

$\mathbf{r}_j = \mathbf{r}_{\text{II}} + \mathbf{b}_{ij}$	J_{ij}	\mathbf{D}_{ij}	$\boldsymbol{\rho}_j$
$-\frac{1}{2} + z_{\text{II}}, \frac{1}{2} - x_{\text{II}}, 1 - y_{\text{II}}$	J_1	D_{1x}, D_{1y}, D_{1z}	$\rho_{\text{II},z}, -\rho_{\text{II},x}, -\rho_{\text{II},y}$
$\frac{1}{2} - y_{\text{II}}, 1 - z_{\text{II}}, \frac{1}{2} + x_{\text{II}}$	J_1	$D_{1y}, D_{1z}, -D_{1x}$	$-\rho_{\text{II},y}, -\rho_{\text{II},z}, \rho_{\text{II},x}$
$-1 + x_{\text{I}}, -1 + x_{\text{I}}, x_{\text{I}}$	J_2	D_{2x}, D_{2y}, D_{2z}	$\rho_{\text{I},x}, \rho_{\text{I},x}, \rho_{\text{I},x}$
$-1 + z_{\text{II}}, x_{\text{II}}, 1 + y_{\text{II}}$	J_3	D_{3x}, D_{3y}, D_{3z}	$\rho_{\text{II},z}, \rho_{\text{II},x}, \rho_{\text{II},y}$
$y_{\text{II}}, -1 + z_{\text{II}}, 1 + x_{\text{II}}$	J_3	$-D_{3y}, -D_{3z}, -D_{3x}$	$\rho_{\text{II},y}, \rho_{\text{II},z}, \rho_{\text{II},x}$
$1 - x_{\text{I}}, -\frac{1}{2} + x_{\text{I}}, \frac{3}{2} - x_{\text{I}}$	J_4	D_{4x}, D_{4y}, D_{4z}	$-\rho_{\text{I},x}, \rho_{\text{I},x}, -\rho_{\text{I},x}$
$\frac{1}{2} - x_{\text{I}}, 1 - x_{\text{I}}, -\frac{1}{2} + x_{\text{I}}$	J_5	D_{5x}, D_{5y}, D_{5z}	$-\rho_{\text{I},x}, -\rho_{\text{I},x}, \rho_{\text{I},x}$

correspondingly. Tilt vectors of other copper atoms can be obtained from these two vectors using symmetry transformations of the point group 23.

Let us use condition (28) for the atoms in positions \mathbf{r}_{I} and \mathbf{r}_{II} , in order to find exchange coordinates of the positions. Then, the system of linear equations can be easily obtained and solved:

$$\mathcal{A} \begin{pmatrix} x_{\text{I}} \\ x_{\text{II}} \\ y_{\text{II}} \\ z_{\text{II}} \end{pmatrix} = \begin{pmatrix} -2J_2 - 3J_4 - 2J_5 \\ -J_2 + J_3 + J_4 + \frac{1}{2}J_5 \\ -\frac{3}{2}J_1 - J_2 + J_3 - \frac{1}{2}J_4 + J_5 \\ -\frac{3}{2}J_1 - 2J_3 + \frac{3}{2}J_4 - \frac{1}{2}J_5 \end{pmatrix}, \quad (50)$$

with

$$\mathcal{A} = \begin{pmatrix} A_{11} & A_{12} & A_{13} & A_{14} \\ -A_{12} & A_{22} & A_{23} & A_{24} \\ -A_{13} & A_{23} & A_{22} & A_{23} \\ -A_{14} & A_{24} & A_{23} & A_{22} \end{pmatrix} \quad (51)$$

$$\begin{aligned} A_{11} &= -3J_2 - 3J_4 - 3J_5 \\ A_{12} &= J_2 - J_4 - J_5 \\ A_{13} &= J_2 + J_4 - J_5 \\ A_{14} &= J_2 - J_4 + J_5 \\ A_{22} &= -2J_1 + J_2 - 2J_3 + J_4 + J_5 \\ A_{23} &= -J_1 + J_3 \\ A_{24} &= J_1 + J_3. \end{aligned} \quad (52)$$

General solution is rather combersome. Using the values of J_1 – J_5 from table 1, we find

$$\begin{aligned} x_{\text{I,exch}} &= 0.9417, \\ x_{\text{II,exch}} &= -0.0042, \\ y_{\text{II,exch}} &= 0.0202, \\ z_{\text{II,exch}} &= 0.8969. \end{aligned} \quad (53)$$

Just these ideal coordinates, rather than the real ones, should be used in calculations of the phenomenological constants \mathcal{J} , \mathcal{D} by formulae (38), (39). The calculation with

the data from table 1 gives $\mathcal{J} = 2.565$ meV, $\mathcal{D} = 0.970$ meV. Therefore, the helix propagation number $k = \mathcal{D}/2\mathcal{J} = 0.1890$ ($q = k/2\pi = 0.0301$). The positive value of k means that the magnetic helicoid is expected to be right-handed in the crystals with the given set of atomic positions. In the enantiomorphs with opposite values of all atomic positions the helicoid should be also opposite (left-handed). This prediction is rather easy for experimental proof (the corresponding procedure is well developed for MnSi-type crystals [29, 30, 31, 32, 33]).

In order to find the tilt vectors, we write system (31) for the atoms in positions \mathbf{r}_I and \mathbf{r}_{II} ,

$$\mathcal{A} \begin{pmatrix} \rho_{I,x} \\ \rho_{II,x} \\ \rho_{II,y} \\ \rho_{II,z} \end{pmatrix} = \begin{pmatrix} B_1 \\ B_2 \\ B_3 \\ B_4 \end{pmatrix} \quad (54)$$

$$\begin{aligned} B_1 &= D_{2x} + D_{2y} + D_{2z} - D_{4x} + D_{4y} - D_{4z} \\ &\quad - D_{5x} - D_{5y} + D_{5z} \\ B_2 &= -D_{1x} - D_{1y} + D_{2x} - D_{3x} + D_{3y} + D_{4x} + D_{5x} \\ B_3 &= -D_{1y} - D_{1z} + D_{2y} - D_{3y} + D_{3z} + D_{4y} + D_{5y} \\ B_4 &= D_{1x} - D_{1z} + D_{2z} + D_{3x} - D_{3z} + D_{4z} + D_{5z}. \end{aligned} \quad (55)$$

Using the data from table 1, we find

$$\begin{aligned} \rho_{I,x} &= 0.049, \\ \rho_{II,x} &= -0.123, \\ \rho_{II,y} &= -0.034, \\ \rho_{II,z} &= -0.159. \end{aligned} \quad (56)$$

The canting angles are $|\boldsymbol{\rho}_I| = 0.084$ (4.8°), $|\boldsymbol{\rho}_{II}| = 0.204$ (11.7°).

The tilt vectors (56) determine spin cantings $\mathbf{u}^{(1)}$ of the first approximation, both in arbitrary twisted phases, including helicoids and A-phase, and in the state unwound by magnetic field $H \gtrsim H_{c2}$. For example, figure 5 shows the canting arrangement in the periodic structure, if the external magnetic field is along the $[001]$ axis. In the first approximation, all cantings lie in plane (001) , perpendicular to the field and magnetization. It is obvious that the canting arrangement is symmetrical relative to the 2_1 screw axes directed along the field.

The absolute atomic configuration of Cu_2OSeO_3 was determined in [28]. We find that it is very close to $P4_132$ cubic symmetry [34], see table 4 where the idealized structure with the $P4_132$ symmetry is compared with the observed structure. Thus, similar to the case of the $B20$ structures [29], we can say that this atomic structure is right-handed because the space group $P4_132$ contains only right-handed screw axes 4_1 . And in this right-handed structure the magnetic helicoids are expected to be right-handed according to above calculations. For another enantiomorph with inverse values of all atomic coordinates, the idealized atomic structure is left-handed ($P4_332$ space group). The corresponding inverted real structure (it has exactly the same energy as

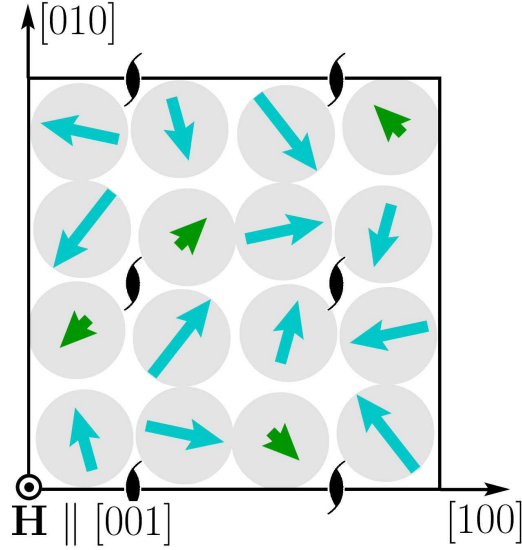


Figure 5. The spin canting in the ferrimagnetic state of Cu_2OSeO_3 , induced by an external magnetic field applied in the $[001]$ direction. The centres of the grey circles coincide with projections of copper atoms in plane (001) . The green and cyan arrows show directions and magnitudes of spin cantings of 4 Cu-I and 12 Cu-II atoms, correspondingly.

Table 4. The atomic structure of Cu_2OSeO_3 [28] with $P2_13$ symmetry and the idealized structure with $P4_132$ symmetry.

atoms	$P2_13$, [28]		$P4_132$	
	type	x, y, z	type	x, y, z
Cu-I	$4a$	0.8860, 0.8860, 0.8860	$4b$	$\frac{7}{8}, \frac{7}{8}, \frac{7}{8}$
Cu-II	$12b$	0.1335, 0.1211, -0.1281	$12d$	$y + \frac{1}{4}, \frac{1}{8}, y$ ($y \approx -0.12$)
Se-I	$4a$	0.4590, 0.4590, 0.4590	$\} 8c$	x, x, x ($x \approx 0.5$)
Se-II	$4a$	0.2113, 0.2113, 0.2113		
O-I	$4a$	0.0105, 0.0105, 0.0105	$\} 8c$	x, x, x ($x \approx 0.0$)
O-II	$4a$	0.7621, 0.7621, 0.7621		
O-III	$12b$	0.2699, 0.4834, 0.4706	$12d$	$-y, y + \frac{3}{4}, \frac{3}{8}$ ($y \approx -0.27$)
O-IV	$12b$	0.2710, 0.1892, 0.0313	$12d$	$y + \frac{1}{4}, \frac{1}{8}, y$ ($y \approx 0.03$)

the structure determined in [28]) can be also considered as left-handed and its magnetic helicoid is expected to be left-handed, but its space group remains $P2_13$.

Another geometrical approach is to reduce the magnetic structure of Cu_2OSeO_3 to that of the MnSi-type crystals [35]. For that, the structure is divided into “strong” tetrahedra of copper atoms, with the summary magnetic moments being considered as individual classical spins. Indeed, as is seen from table 1, the bonds 2 and 3 have the maximal absolute values of the exchange interaction constants. The approximation of strong tetrahedra corresponds to the infinite constants: $J_2 = -\infty$, $J_3 = +\infty$. Then, the corresponding bonds with the exchange coordinates become zero, $\mathbf{b}_2 = \mathbf{b}_3 = 0$, and

the tetrahedra transform to “atoms” in positions $4a$ with coordinate

$$x_{\text{exch}} \equiv x_{\text{I,exch}} - 1 = x_{\text{II,exch}} = y_{\text{II,exch}} = z_{\text{II,exch}} - 1. \quad (57)$$

Besides, the bonds \mathbf{b}_1 of Cu_2OSeO_3 transform into the bonds \mathbf{b}_1 of MnSi, whereas the bonds \mathbf{b}_4 and \mathbf{b}_5 of Cu_2OSeO_3 become the bonds \mathbf{b}_3 of MnSi. The coordinate x_{exch} can be found from the solution of the system (50), when passing to the limit $J_2 \rightarrow -\infty$, $J_3 \rightarrow +\infty$. But, it is easier to use expression (43) for MnSi with the parameters $J_1(\text{MnSi}) = J_1(\text{Cu}_2\text{OSeO}_3)$, $J_2(\text{MnSi}) = 0$, and $J_3(\text{MnSi}) = -(J_4 + J_5)(\text{Cu}_2\text{OSeO}_3)$ (the sign minus is due to bonds \mathbf{b}_4 and \mathbf{b}_5 connecting atoms Cu-I and Cu-II having opposite spins). Therefore,

$$x_{\text{exch}} = \frac{J_1 + J_4 + J_5}{8(J_1 - J_4 - J_5)}(\text{Cu}_2\text{OSeO}_3) = -0.0312. \quad (58)$$

Then, from (38)–(40) can be calculated $\mathcal{J} = 2.969$ meV, $\mathcal{D} = 0.534$ meV, and $k = 0.0900$. As we see, the approximation of “strong” tetrahedra with the data from [19] gives value of the propagation number k , which is two times less than one obtained with true energetic parameters of bonds \mathbf{b}_2 and \mathbf{b}_3 .

9. Discussion

The calculated value of the propagation number, $k = 0.189$, is almost three times greater than one found in [19] without taking the canting into account, and approximately two times bigger than the experimental value $k = 0.088$ [9, 10]. Let us explain the cause of it. In order to calculate k in the one-helix model (without canting), the formulae (38)–(40) can be used with real coordinates instead of exchange ones. Indeed, in this case, using the data from [19], we find $k = 0.07$, which is very close to the value calculated in [19] without taking the canting into account. In order to understand this essential difference, notice that, accordingly to (39), the phenomenological parameter \mathcal{D} determining spiralling of the magnetic structure is composed of the scalar products $\mathbf{D} \cdot \mathbf{b}$. It is well known from the superexchange theory, that the DM vectors are approximately perpendicular to the bonds (see also third column in table 5). Were the perpendicularity of the DM vectors to the bonds exact, the spiralling would be absent on condition that expression (39) contained vectors \mathbf{b} with real coordinates. However, the expression depends on the exchange ones, and, consequently, \mathcal{D} is a linear combination of differences $x_{\text{exch}} - x_{\text{real}}$ with coefficients from the DM vector components. Therefore, the exact numerical values of x_{exch} can strongly affect the spiralling, determining both pitch and sense of the magnetic helix.

In table 5, the calculated with the use of (53) lengths of the “exchange” bonds \mathbf{b}_e are listed. As one can see, the lengths $|\mathbf{b}_e|$ of the 2nd and the 3rd bonds are considerably less than the real ones. It rather justifies the approximation of strong tetrahedra [35], in which $\mathbf{b}_2 = \mathbf{b}_3 = 0$. Another important factor is the angle between the DM vector and the bond \mathbf{b}_e in exchange coordinates. From table 5 it is seen that, in accordance with [19], the angles $\angle(\mathbf{b}_r, \mathbf{D})$ are really close to 90° . But, in exchange coordinates, the

differences of $\angle(\mathbf{b}_e, \mathbf{D})$ from the right angle is more considerable, particularly for the 2nd and the 3rd bonds.

Table 5. The changing of bond lengths and directions, when replacing the real coordinates by the exchange ones. The energetic parameters of bonds $\mathbf{b}_1, \dots, \mathbf{b}_5$ are listed in [19] and table 1. The real (\mathbf{b}_r) and “exchange” (\mathbf{b}_e) bonds are calculated by the substitution of the coordinates from [28] and equation (53), respectively.

	$ \mathbf{b}_r $	$\angle(\mathbf{b}_r, \mathbf{D})$	$ \mathbf{b}_e $	$\angle(\mathbf{b}_e, \mathbf{D})$	$\angle(\mathbf{b}_e, \mathbf{b}_r)$
\mathbf{b}_1	0.3422	94.3°	0.6340	99.5°	7.8°
\mathbf{b}_2	0.3417	85.3°	0.1053	71.3°	25.5°
\mathbf{b}_3	0.3615	99.5°	0.1599	110.2°	13.2°
\mathbf{b}_4	0.3702	86.3°	0.5443	83.8°	11.0°
\mathbf{b}_5	0.7114	85.8°	0.6325	86.9°	5.0°

The significant difference between experimental and calculated values of propagation number can result from (i) an inaccuracy of *ab initio* calculations of the bond parameters J_{ij} and \mathbf{D}_{ij} , (ii) the neglect of other bonds from the second and next magnetic shells, (iii) the presence of a non-isotropic interaction different from Dzyaloshinskii–Moriya one. It is important here to attend to the calculation accuracy of DM vector projections on the bond directions (in exchange coordinates), because only these projections affect the twist. If vectors \mathbf{D}_{ij} are almost perpendicular to bonds, then their projections on the bond directions are relatively small in size, and even a slight change of their values can have a strong influence on the phenomenological constant \mathcal{D} and consequently on the propagation number k . On the other hand, the isotropic parameters J_{ij} can provide their influence both through the phenomenological constant \mathcal{J} and the exchange coordinates. It is noteworthy, that although J_{ij} and \mathbf{D}_{ij} decrease with distance, their contributions into the macroscopic parameters \mathcal{J} and \mathcal{D} , accordingly to (38) and (39), are proportional to b_{ij}^2 and b_{ij} , correspondingly. Moreover, the number of neighbours also increases with distance. Thus, for example, there are eight non-equivalent bonds in the second magnetic environment ranging from 5.35 to 5.54 Å.

As can be seen from (53), the maximal deviation of the exchange coordinate from the real one is for x_{II} , $|x_{\text{II,exch}} - x_{\text{II,real}}| = 0.14$. In [27] it is shown that for itinerant magnetics of the MnSi-type in the frame of RKKY model, x_{exch} can have practically any value (we would remind that the ideal coordinates are nothing but some functions of the exchange parameters J_{ij}). Nevertheless, some limitation can result from the condition of validity of the theory. In order to study this we should first understand the origin of the exchange coordinates. When a transition is performed from discrete spins to continuous magnetic moment, some frustrations appear from the fact that the spins correspond poorly to the values of smooth function (e.g. helicoid) in their physical positions. It is just the cause why, accordingly to equation (12), two kinds of canting can be distinguished: the first one determined by the DM interaction, and the

second one connected with spatial derivatives. The latter is due to existence of several magnetic helices, with small phase shifts from the average single helix. The appropriate displacement of the magnetic atoms into the fictitious positions (which does not influence the magnetic energy) makes all the individual helices confluent, and the canting due to spatial derivatives disappears (figure 6). In fact, the small deviation $x_{\text{exch}} - x_{\text{real}}$ of the exchange coordinate from the real one for Cu_2OSeO_3 means that the phase shifts of the individual helices are also small, which correlates with the assumption about small cantings between neighbouring spins. Greater phase shifts would mean that we could not already consider the spins as weak non-collinear, and the simplifications of section 5 would be impossible.

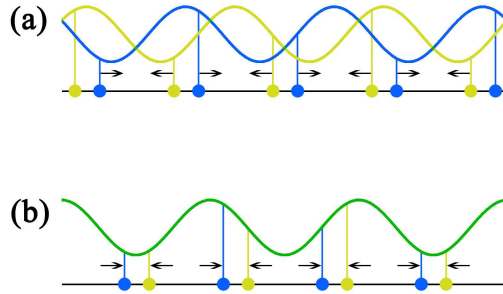


Figure 6. (a) In the real spin structure there are several magnetic helices, corresponding to different magnetic atoms in the unit cell, with phase shifts between them. (b) When the atoms “move” (arrows) from the real positions to the fictitious (exchange) ones, the phase shifts disappear and the helices become confluent.

Another important property is the sense of the magnetic chirality. In the case when a twist arises from a spontaneous break of symmetry, the helix sense can be plus or minus with equal probability and in each case it is casual. In contrast, for the magnetics without centre of inversion, exemplified by MnSi , Cu_2OSeO_3 and other crystals, the sense of the magnetic chirality correlates with the structural one. Thus, in pure MnSi , the left-handed atomic structure results in the left-handed magnetic helix [30, 31]. Besides, the chiral interlink in MnSi -type helimagnetics is found to be strongly dependent on their atomic composition [27, 29, 32, 33]. In the present work, using the magnetic data from [19], we obtain $k = 0.189$, i.e. the helicoid is right for the structure described in [28] and used in simulations of [19]. Recently, this important result has been experimentally proved by Dyadkin *et al.* [36].

In the first approximation, the cantings, being only small corrections to spins, are perpendicular to the latters. Consequently, the cantings of all N magnetic atoms in the unit cell are determined by $2N$ variables. Thus, for Cu_2OSeO_3 the number of canting components amounts to 32 per unit cell. Surprisingly, that, owing the (tetrahedral) symmetry of the crystal, we can make with a considerably lower number of parameters in order to describe the local magnetic structure: four exchange coordinates $x_{\text{I,exch}}$, $x_{\text{II,exch}}$, $y_{\text{II,exch}}$, $z_{\text{II,exch}}$, and four tilt vector components $\rho_{\text{I},x}$, $\rho_{\text{II},x}$, $\rho_{\text{II},y}$, $\rho_{\text{II},z}$. For MnSi -

type helimagnetics there are only two parameters: x_{exch} and ρ_x .

In (56), the values of tilt vectors $\boldsymbol{\rho}$ are calculated with the use of energetic parameters J , \mathbf{D} from [19]. In addition to the propagation number k , given by (40), these, characterizing the canting, vectors are the experimentally observed parameters of the magnetic structure. In [25] the conditions were proposed of a diffraction experiment to find the canting in the MnSi-type helimagnets. Because the magnetic atoms in these crystals are situated at the special positions $4a$, the tilt vectors are defined by only one parameter ρ_x , which is proposed to be found in the measurement of the “forbidden” Bragg reflection 00ℓ , $\ell = 2n + 1$ in the unwound by magnetic field structure. In the general case of cubic helimagnets with almost collinear spins, the antiferromagnetic (canting) part of the structure factor is determined by the vector

$$\Phi = \sum_i c_i \boldsymbol{\rho}_i \exp(i\mathbf{Q} \cdot \mathbf{r}_i), \quad (59)$$

where $\mathbf{Q} = 2\pi(hk\ell)$ is a reflection vector, and summation is taken over all magnetic atoms in the unit cell. In particular, for the copper atoms in the general positions $12b$ and the pure magnetic reflection 00ℓ , $\ell = 2n + 1$, this sum has the view

$$\begin{aligned} \Phi = 4(\rho_y \cos 2\pi\ell x + \rho_z \cos 2\pi\ell y + \rho_x \cos 2\pi\ell z, \\ i\rho_z \sin 2\pi\ell x + i\rho_x \sin 2\pi\ell y + i\rho_y \sin 2\pi\ell z, 0). \end{aligned} \quad (60)$$

It is obvious that, in order to find all components of tilt vectors $\boldsymbol{\rho}$ for magnetic atoms in all non-equivalent positions, several forbidden reflections with different ℓ should be measured.

Notice that, as far as the measurable parameters k , $\boldsymbol{\rho}$ are determined by greater number of constants J_{ij} , \mathbf{D}_{ij} , the problem of finding of the latter from experimental data is unsolvable in general. At the best, only some combinations of J and \mathbf{D} can be calculated by inversion of equations (40) and (54). Nevertheless, the comparison of theoretical predictions with measurements can confirm (or refute) reliability of *ab initio* calculations of the energetic parameters.

Acknowledgments

We are grateful to O. Janson, A. A. Tsirlin and S. S. Doudoukine for useful discussions and encouragement and to J. H. Yang, H. J. Xiang and X. G. Gong for providing us with details of their DFT calculations of the exchange parameters and the DM vectors in Cu_2OSeO_3 . The reported study was partially supported by RFBR, research project No. 14-02-00268 a, and by two projects of the Presidium of the Russian Academy of Sciences: “Matter at high energy densities; Substance under high static compression” and “Diffraction of synchrotron radiation in multiferroics and chiral magnetics”.

References

- [1] Grigoriev S V, Maleyev S V, Okorokov A I, Chetverikov Yu O, Böni P, Georgii R, Lamago D, Eckerlebe H and Pranzas K 2006 Magnetic structure of MnSi under an applied field probed by polarized small-angle neutron scattering *Phys. Rev. B* **74** 214414
- [2] Mühlbauer S, Binz B, Jonietz F, Pfleiderer C, Rosch A, Neubauer A, Georgii R and Böni P 2009 Skyrmion lattice in a chiral magnet *Science* **323** 915–9
- [3] Münzer W *et al* 2010 Skyrmion lattice in the doped semiconductor $\text{Fe}_{1-x}\text{Co}_x\text{Si}$ *Phys. Rev. B* **81** 041203
- [4] Adams T *et al* 2011 Long-range crystalline nature of the skyrmion lattice in MnSi *Phys. Rev. Lett.* **107** 217206
- [5] Bogdanov A N and Yablonskii D A 1989 Thermodynamically stable “vortices” in magnetically ordered crystals. The mixed state of magnets *Sov. Phys.-JETP* **68** 101–3
- [6] Rößler U K, Bogdanov A N and Pfleiderer C 2006 Spontaneous skyrmion ground states in magnetic metals *Nature* **442** 797–801
- [7] Ambrose M C and Stamps R L 2013 Melting of hexagonal skyrmion states in chiral magnets *New J. Phys.* **15** 053003
- [8] Seki S, Yu X Z, Ishiwata S and Tokura Y 2012 Observation of skyrmions in a multiferroic material *Science* **336** 198–201
- [9] Adams T, Chacon A, Wagner M, Bauer A, Brandl G, Pedersen B, Berger H, Lemmens P and Pfleiderer C 2012 Long-wavelength helimagnetic order and skyrmion lattice phase in Cu_2OSeO_3 *Phys. Rev. Lett.* **108** 237204
- [10] Seki S, Kim J-H, Inosov D S, Georgii R, Keimer B, Ishiwata S and Tokura Y 2012 Formation and rotation of skyrmion crystal in the chiral-lattice insulator Cu_2OSeO_3 *Phys. Rev. B* **85** 220406(R)
- [11] Onose Y, Okamura Y, Seki S, Ishiwata S and Tokura Y 2012 Observation of magnetic excitations of skyrmion crystal in a helimagnetic insulator Cu_2OSeO_3 *Phys. Rev. Lett.* **109** 037603
- [12] Seki S, Ishiwata S and Tokura Y 2012 Magnetoelectric nature of skyrmions in a chiral magnetic insulator Cu_2OSeO_3 *Phys. Rev. B* **86** 060403(R)
- [13] White J S *et al* 2012 Electric field control of the skyrmion lattice in Cu_2OSeO_3 *J. Phys.: Condens. Matter* **24** 432201
- [14] Bos J-W G, Colin C V and Palstra T T M 2008 Magnetoelectric coupling in the cubic ferrimagnet Cu_2OSeO_3 *Phys. Rev. B* **78** 094416
- [15] Miller K H, Xu X S, Berger H, Knowles E S, Arenas D J, Meisel M W and Tanner D B 2010 Magnetodielectric coupling of infrared phonons in single-crystal Cu_2OSeO_3 *Phys. Rev. B* **82** 144107
- [16] Maisuradze A, Guguchia Z, Graneli B, Rønnow H M, Berger H and Keller H 2011 μSR investigation of magnetism and magnetoelectric coupling in Cu_2OSeO_3 *Phys. Rev. B* **84** 064433
- [17] Maisuradze A, Shengelaya A, Berger H, Djokić D M and Keller H 2012 Magnetoelectric coupling in single crystal Cu_2OSeO_3 studied by a novel electron spin resonance technique *Phys. Rev. Lett.* **108** 247211
- [18] Belesi M, Rousochatzakis I, Abid M, Rößler U K, Berger H and Ansermet J-Ph 2012 Magnetoelectric effects in single crystals of the cubic ferrimagnetic helimagnet Cu_2OSeO_3 *Phys. Rev. B* **85** 224413
- [19] Yang J H, Li Z L, Lu X Z, Whangbo M-H, Su-Huai Wei, Gong X G and Xiang H J 2012 Strong Dzyaloshinskii-Moriya interaction and origin of ferroelectricity in Cu_2OSeO_3 *Phys. Rev. Lett.* **109** 107203
- [20] Ye-Hua Liu, You-Quan Li and Jung Hoon Han 2013 Skyrmion dynamics in multiferroic insulators *Phys. Rev. B* **87** 100402(R)
- [21] Ye-Hua Liu and You-Quan Li 2013 A mechanism to pin skyrmions in chiral magnets *J. Phys.: Condens. Matter* **25** 076005
- [22] Jennings P and Sutcliffe P 2013 The dynamics of domain wall Skyrmions *J. Phys. A: Math. Theor.*

46 465401

- [23] Pyatakov A P and Zvezdin A K 2012 Magnetoelectric and multiferroic media *Physics–Uspekhi* **55** 557–81
- [24] Morrish A H 1994 *Canted Antiferromagnetism: Hematite* (Singapore: World Scientific)
- [25] Dmitrienko V E and Chizhikov V A 2012 Weak antiferromagnetic ordering induced by Dzyaloshinskii-Moriya interaction and pure magnetic reflections in MnSi-type crystals *Phys. Rev. Lett.* **108** 187203
- [26] Chizhikov V A and Dmitrienko V E 2012 Frustrated magnetic helices in MnSi-type crystals *Phys. Rev. B* **85** 014421
- [27] Chizhikov V A and Dmitrienko V E 2013 Multishell contribution to the Dzyaloshinskii-Moriya spiraling in MnSi-type crystals *Phys. Rev. B* **88** 214402
- [28] Effenberger H and Pertlik F 1986 Die kristallstrukturen der kupfer(II)-oxo-selenite $\text{Cu}_2\text{O}(\text{SeO}_3)$ (kubisch und monoklin) und $\text{Cu}_4\text{O}(\text{SeO}_3)_3$ (monoklin und triklin) *Monatsh. Chem.* **117** 887–96
- [29] Dmitriev V, Chernyshov D, Grigoriev S and Dyadkin V 2012 A chiral link between structure and magnetism in MnSi *J. Phys.: Condens. Matter* **24** 366005
- [30] Tanaka M, Takayoshi H, Ishida M and Endoh Ya 1985 Crystal chirality and helicity of the helical spin density wave in MnSi. I. Convergent-beam electron diffraction *J. Phys. Soc. Japan* **54** 2970–4
- [31] Ishida M, Endoh Ya, Mitsuda S, Ishikawa Yo and Tanaka M 1985 Crystal chirality and helicity of the helical spin density wave in MnSi. II. Polarized neutron diffraction *J. Phys. Soc. Japan* **54** 2975–82
- [32] Grigoriev S V *et al* 2013 Chiral properties of structure and magnetism in $\text{Mn}_{1-x}\text{Fe}_x\text{Ge}$ compounds: When the left and the right are fighting, who wins? *Phys. Rev. Lett.* **110** 207201
- [33] Shibata K, Yu X Z, Hara T, Morikawa D, Kanazawa N, Kimoto K, Ishiwata S, Matsui Y and Tokura Y 2013 Towards control of the size and helicity of skyrmions in helimagnetic alloys by spinorbit coupling *Nature Nanotechnol.* **8** 723–8
- [34] Hahn T (ed) 1989 *International Tables for Crystallography, Vol. A: Space-Group Symmetry* (Dordrecht, The Netherlands: Kluwer Academic)
- [35] Janson O, Rouschatzakis I, Tsirlin A A, Rößler U K, van den Brink J and Rosner H 2013 Microscopic modeling of the $S=1/2$ Heisenberg ferrimagnet Cu_2OSeO_3 *Int. Workshop “Dzyaloshinskii–Moriya Interaction and Exotic Spin Structures” (Veliky Novgorod, Russia)* (Gatchina: Petersburg Nuclear Physics Institute) p 67
- [36] Dyadkin V, Grigoriev S V, White J S, Prša K, Huang P, Rønnow H, Magrez A, Dewhurst C D and Chernyshov D 2014 Chirality of structure and magnetism in the magnetoelectric Cu_2OSeO_3 (in press)